EUROPEAN ORGANIZATION FOR NUCLEAR RESEARCH

Proposal to the ISOLDE and Neutron Time-of-Flight Committee

Proton resonance elastic scattering of ^{30}Mg for single particle structure of ^{31}Mg

October 6, 2011

N. Imai[1], J. Cederkall[2], Y. Hirayama[1], H. Ishiyama[1], S.C. Jeong[1], S. Kubono[3], H. Miyatake[1], T. Teranishi[4], Y.X. Watanabe[1], H. Yamaguchi[3]

[1]*Institute of Particle and Nuclear study, High Energy Accelerator Research Organization (KEK), Oho 1-1, Tsukuba, Ibaraki 305-0801, Japan*
[2]*Physics Department, Lund University, SE-221 00, Lund, Sweden*
[3]*Center for Nuclear Study, University of Tokyo, RIKEN campus, Hirosawa 2-1, Wako, Saitama 351-0198, Japan*
[4]*Department of Physics, Kyushu University, Fukuoka 812-8581, Japan*

Spokesperson: N. imai/ nobuaki.imai@kek.jp
Contact person: J. Cerderkall/ joakim.cerderkall@nuclear.lu.se

CERN-INTC-2011-044 / INTC-P-308
06/10/2011

Abstract

The single particle structure of ^{31}Mg, which are located in the so-called "island of inversion", will be studied through measuring Isobaric Analog Resonances (IARs) of bound states of ^{31}Mg. They are located in the high excitation energy of ^{31}Al. We are going to determine the spectroscopic factors and angular momenta of the parent states by measuring the excitation function of the proton resonance elastic scattering around 0 degrees in the laboratory frame with around 3 MeV/nucleon ^{30}Mg beam. The present study will reveal the shell evolution around ^{32}Mg. In addition, the spectroscopic factor of the $7/2^-$ state which were not yet determined experimentally, has possibility to discuss the shape coexistence in this nucleus.

Requested shifts: [10] shifts, (split into [1] runs over [1] years)

1 Physics background

Around neutron-rich nuclei around ^{32}Mg, the neutron fp orbitals are replaced with the sd orbitals, leading to disappearance of the neutron magic number $N = 20$. Many experimental efforts have been devoted to understand the shell structure by using quadrupole collectivity [1, 2, 3], β decay [4, 5], mass measurement [6], and so on. However, the single particle structure of this region has not yet been studied although it is directly related to the variation of the shell structure.

The systematics of the low lying levels of $N = 19$ isotones are shown in Fig. 1. From the simple shell model picture, the energy of the $7/2^-$ state suggests the shell gap of $N = 20$. Indeed, the energy of the state decreases from 2.8 MeV to 1.5 MeV when the proton number (Z) changes from 20 to 14. Eventually, in the ^{31}Mg, the candidate of the state is located at 461 keV [7, 8] which were not experimentally confirmed. Determination of the place of the $7/2^-$ state in ^{31}Mg reveals the evolution of the state in $N = 19$ isotopes.

The spectroscopic factor of the state will give us further insight of an exotic phenomena. A low-lying second 0^+ state in ^{32}Mg which was recently observed suggests the shape coexistence in the nucleus [9]. Such phenomenon should be observed in ^{31}Mg since the ground state of ^{31}Mg is considered to be deformed [10] as suggested by the g-factor of the state. In the Nilson diagram, as deformation proceeds, the single particle energy of the $7/2^-$ state increases. The low-lying $7/2^-$ state suggests that the single particle state coupled to a spherical core nucleus. On the other hand, $J^\pi = 7/2^-$ can be generated by ^{30}Mg$(2^+) + 3/2^-$ as well as ^{30}Mg$(0^+) + 7/2^-$. The former configuration can be considered as a deformed state, while the latter as a spherical one. The spectroscopic factor of the state gives us a hint of the shape coexistence in the ^{31}Mg [11].

2 Experiment

2.1 Isobaric Analog Resonance

We aim at experimentally determining the spectroscopic factors and angular momenta of the low-lying states in ^{31}Mg. One of the standard ways to investigate the neutron

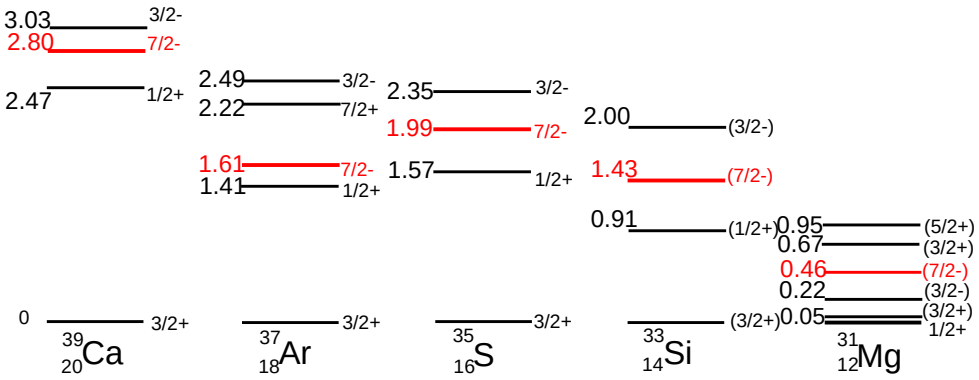

Figure 1: Systematics of low-lying excited states in the $N = 19$ isotones.

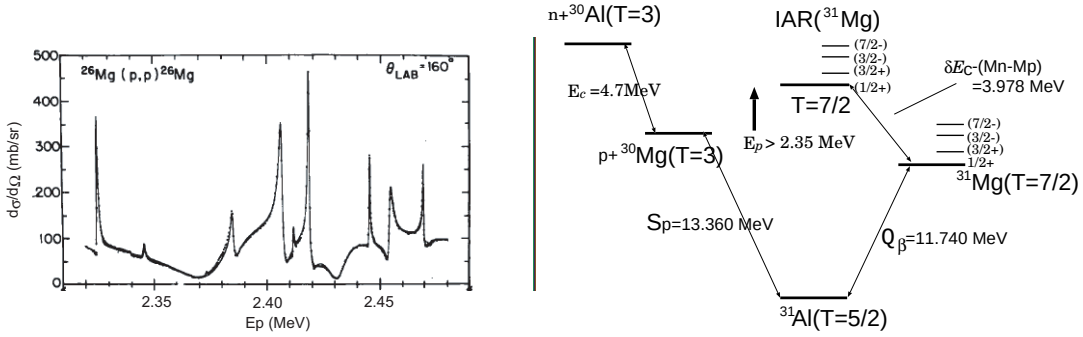

Figure 2: (left) Typical example of IAR measurement by proton elastic scattering. Several IARs were measured by the ^{26}Mg(p,p)^{26}Mg reaction at 160 degrees [12]. (right) Energy scheme of $A = 31$ system. Sp, δE_c, Q_β stand for proton separation energy, Coulomb energy difference, Q value for the β decay, respectively.

single particle wave function is measurement of the neutron transfer reaction, e.g. (d, p) reaction. However, in the case of the (d, p) reaction under the inverse kinematics condition, the proton energies scattered at forward angles in the center of mass (c.m.) frame are often very small, typically about 1 MeV. And thus, in the case of the high level density, especially in massive nuclei, it is difficult to distinguish the excited states by measuring the recoil proton energies without a spectrograph. As an alternative way, we propose here a measurement of isobaric analog resonances (IARs) which locate at high excited state of the neighboring isobar. Assuming the isospin symmetry of the nuclear force, a spectroscopic factor and J^π of a nuclear state of interest are identical with those for a corresponding IAR.

The IAR can be observed through measuring the excitation function of elastic scattering of protons at a backward angle in the c.m. frame. When a reaction energy in the c.m. frame $E_{c.m.}$ is identical with a resonance energy, the cross section of elastic scattering is enhanced. The shape of the resonance depends on the orbital angular momentum l, while the peak height reflects the spectroscopic factor. Under the inverse kinematics condition, the proton energy will be about 4 times larger than the $E_{c.m.}$. Since the level densities in the rest frame is also magnified to be 4 times in the proton energy spectrum, we can easily distinguish the levels.

A typical example of the IAR measurement is shown in Fig. 2. Several IARs of ^{27}Mg were clearly observed through measuring protons elastically scattered at 160 degrees on ^{26}Mg [12]. In the experiment, the resonances were searched for by changing the proton beam energy. The IAR of ^{27}Mg($J^\pi = 7/2^-$) was measured with 2.32-MeV proton. The R-matrix analysis yielded that both total width ($\Gamma_{\rm tot.}$) and proton width (Γ_p) are 0.12 keV. Note that for almost all IARs $\Gamma_{\rm tot.} \simeq \Gamma_p$ was obtained in the experiment.

The energy level scheme of $A = 31$ system is shown in the right of Fig. 2. The IAR of ^{31}Mg(g.s.) is expected to be placed at the excitation energy of 15.718 MeV in ^{31}Al. The excitation energy is determined by the Coulomb energy difference δE_c and the mass difference Q_β [13] between ^{31}Mg and ^{31}Al, and the mass difference between proton (M_p) and neutron (M_n). The δE_c can be estimated using a semi-empirical formula [17]. We're

able to measure the IARs of the bound state of ^{31}Mg through the proton elastic resonance scattering measurement with a reaction energy of $E_{c.m.} \geq 2.3$ MeV. The energy can be estimated by an equation $\delta E_c - (M_n - M_p) + Q_\beta - S_p$. Here, S_p stands for the proton separation energy of ^{35}P. The energy of IAR also gives a useful information on the nuclear structure since the δE_c is associated with the charge radii difference between IARs and the corresponding parent states.

2.2 Estimation of proton width

The Γ_p for IARs of bound states in ^{31}Mg can be estimated using R-matrix calculation with assumed spectroscopic factors. The spectroscopic factors used in this estimation are based on the measured spectroscopic factors of low-lying states in $N = 19$ isotones, ^{35}S [14] and ^{37}Ar [15], listed in Table. 1. The systemics suggests that spectroscopic factors of low-lying states were about 0.2–0.7. For simplicity, here the S is assumed to be 0.3. The R-matrix calculations with the spectroscopic factors yield Γ_p of several 10 keV for the $l = 0, 1, 2$, state, and a few keV for $l = 3$ as presented in Table 2. The quenched Γ_p for $7/2^-$ is mainly attributed to a small penetrability of the high angular momentum.
The calculated excitation function is shown in Fig. 3. Here, we assume $\Gamma_p = \Gamma_{\rm tot.}$. The excitation function is folded with the expected energy resolution of 20 keV in the center of mass frame, which corresponds to the uncertainty of 80 keV in the lab. frame. $E_{c.m.}$ was estimated using the same δE_c and the excitation energies of the respective parent states. Although the first and second peaks cannot be resolved since the excitation energy of the first excited state is as low as 50 keV, other peaks should be clearly separated.
If the J^πs of 3rd and 4th resonances are exchanged, the shape of the curve will change drastically, as shown by the dashed line in Fig. 3. We can identify the resonances clearly.

2.3 Experimental setup

The proton elastic resonance scattering will be measured by an inverse kinematics reaction $p(^{30}\mathrm{Mg},p)^{30}\mathrm{Mg}$. A schematic picture of the experimental setup is shown in Fig. 4. In the experiment, the thick target method [18, 19] is used to efficiently measure the excitation function. A 60 μm thick CH_2 target will be irradiated by a ^{30}Mg beam of 3 MeV/nucleon. The beam itself will stop in the target, and only recoil protons will are emitted from the target.
The reaction point will be deduced assuming elastics scattering and energy losses of the ^{30}Mg and protons in the target. Nevertheless, since the protons lose little energy in the

Table 1: Spectroscopic factors of low-lying excited states in $N = 19$ isotopes

J^π	^{35}S [14]	^{37}Ar [15]
$3/2^+$	0.43	0.56
$1/2^+$	0.15	0.22
$7/2^-$	0.84	0.76
$3/2^-$	0.51	0.44

Table 2: Assigned spin and parities [4], and expected resonance parameters of resonances of IARs corresponding to the low-lying states in ^{31}Mg.

#	Ex (keV)	J^π	$E_{c.m.}$ (MeV)	Γ_p (keV)
1	0.	$1/2^+$	2.307	57.
2	50.	$3/2^+$	2.357	11.
3	221.	$(3/2^-)$	2.528	50.
4	461.	$(7/2^-)$	2.768	6.0
5	673.	$3/2^+$	2.980	27.0
6	945.	$5/2^+$	3.252	27.0

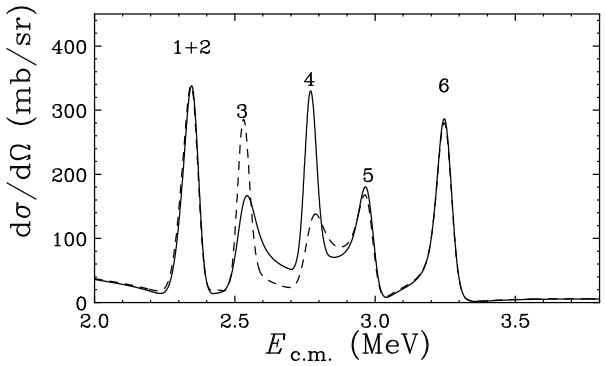

Figure 3: Calculated excitation function for proton elastics scattering of ^{30}Mg assuming the resonance parameters tabulated in Table 2 is shown by the solid line. The dashed line stands for a result when the $3/2^-$ and $7/2^-$ was exchanged.

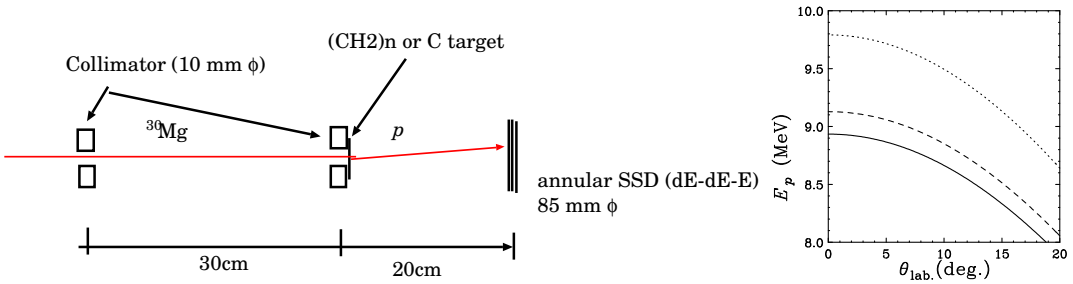

Figure 4: (Left) Schematic view of the experimental setup. (Right) Kinematics. Proton energy as a function of scattering angles for $E_{cm} = 2.307, 2.357$, and 2.528 MeV as solid, dashed, and dotted lines, respectively.

target, measurements of the energies and scattering angles of protons are sufficient to determine the c.m. energy at which the reaction occurred.
We will measure the excitation function of the protons scattered around 0 degrees in the laboratory (lab.) frame, which corresponds to 180 degrees in the c.m. frame. The energy and angular spread due to the multiple scattering for protons in the target are calculated to be 20 keV and 6 mrad, respectively.
The right of Fig. 4 shows the energies of protons as a function of scattering angles. A solid line indicates the proton energy for ^{30}Mg beam of 2.3 MeV/nucleon, where the IAR of the ground state is expected to appear, while a dotted line represents the IAR of 221 keV-excited state ($E_{^{34}\mathrm{Si}}$ = 2.5 MeV/nucleon). The 220 keV discrepancy between the ground and the 2nd excited state is expanded to about 800 keV difference for the recoil proton energy at 0 degrees. Accordingly, $\Gamma_{\mathrm{tot.}}$ and Γ_p in the lab. frame will also be 4 times larger than those values in the c.m. frame. The kinematics indicates that when the scattering angles are smaller than 5.5 degrees, the energy differences of the scattered protons are restricted within 80 (20) keV (σ) in the lab. (c.m.) frame.
A pair of collimators of 1 cm diameter will be installed upstream of the target by 30 cm in order to make sure the incident beam angles. The angular divergence will be restricted within 2 degrees (σ).
The energies of recoil protons will be measured by three layers of annular type silicon telescope, which have 300, 500, 500 μm thicknesses. They will be placed downstream of the target by 20 cm. Scattered particles will be identified by $\Delta E - E$ method. The outer radius is 85 mm in diameter. Their front-sides are divided to 32 rings and backsides are to 64 sectors so that we can determine the scattering angles of protons with the angular resolution of 0.3 degrees. The expected energy resolution for protons is about 80 keV by using three SSDs. The effect of the multiple scattering is negligible for the measured proton energy.

3 Yield estimation

A statistical error of 10% is enough to identify the l of the IAR as shown in Sec.2.4. We'll obtain the statistics with 3 shifts accumulation as described below.

1. **Cross section;** A differential cross section of the elastic scattering for the off-resonance region is calculated to be about 80 mb/sr$_{\mathrm{lab.}}$ at E = 2.5 MeV/nucleon.
2. **Target thickness** d**;** An energy resolution measured by three SSDs is assumed as 80 keV in σ. The resolution corresponds to about 20 keV in c.m. The thickness of the CH_2 target where ^{30}Mg beam loses 20 keV/nucleon is 160 μg/cm^2.
3. **Beam intensity** I**;** We can expect 4×10^4 pps ^{30}Mg beams of a 3 MeV/nucleon from the past experiment [9].
4. **Solid angle** ΔS**;** When the scattering angle is less than 5.5 degrees, the proton energy varies by about 80 keV. The opening angle corresponds to 29 msr.

$\frac{d\sigma}{d\Omega}_{\mathrm{lab.}}$ (mb/sr)	d (g/cm^2)	I (cps)	ΔS (sr)	Yield (cpd/20 keV$_{\mathrm{c.m.}}$)
80.	$160. \times 10^{-6}$	4×10^4	2.9×10^{-2}	110

4 Other reaction channels

1. **(p,p') reaction;** Inelastic scattering at 0 degrees in the lab. frame is negligible since cross sections at 180 degrees in c.m. frame are by 3 order of magnitudes smaller than those for the elastic scattering.
2. **(p,n) reaction;** We can exclude the neutron events by using energy deposit in SSD.
3. **fusion reaction;** Fusion reaction of ^{12}C may contribute to the excitation function of proton. A separate measurement with a ^{12}C target will be performed to evaluate the contribution.

5 Summary of requested shifts:

We would like to 10 shifts in total. For beam transport, we call for 3 shifts. After that we'll start measuring the proton elastics resonance scattering with stable beams of ^{26}Mg and check data acquisition system and so on with 2 shifts. Then, we're going to the radioactive ^{30}Mg for 3 shifts with polyethylene target and 2 shifts with carbon target.

beam transport	3 shifts
^{26}Mg(stable) beam with CH_2 and circuit tuning	2 shifts
^{30}Mg beam with CH_2	3 shifts
^{30}Mg beam with C	2 shifts
total	10 shifts

References

[1] T. Motobayashi *et al.,* Phys. Lett. B **346** (1995) 9.
[2] R.W. Ibbotson *et al.,* Phys. Rev. Lett. **80** (1998) 2081.
[3] B.V. Pritychenko, *et. al.*, Phys. Rev. **C 65** (2002) 061304(R).
[4] C. Thibault, *et. al.*, Phys. Rev. **C 12** (1975) 644.
[5] S. Nummela, *et. al.*, Phys. Rev. **C 64** (2001) 054313.
[6] F. Sarazin *et al.,* Phys. Rev. Lett. **84** (2000) 5062.
[7] G. Klotz, *et al.,* Phys. Rev. C47 (1993) 2502.
[8] H. Mach, *et al.,* Eur. Phys. A 25 (2005) 105.
[9] K. Wimmer, *et al.*, Phys. Rev.Lett. 105, (2010) 252501.
[10] G. Neyens, *et al.*, Phys. Rev. Lett. 94 (2005) 022501.
[11] M. Kimura, private communication.
[12] C. R. Westerfeldt, G. E. Mitchell, E. G. Bilpuch and D. A. Outlaw, Nuclear Physics **A303** (1978) 111.
[13] R.B. Firestone and V.S. Shirley, *Table of Isotopes* (Wiley, New York, 1996), 8th ed., Vol. I.
[14] S. Piskor, P. Franc, J. Kremenek, W. Schäferlingova, Nucl. Phys. A 414 (1984) 219.
[15] S. Sen, W.A. Yoh, and M.T. McEllistrem, Phys. Rev. C 10, (1974) 1050.
[16] Ole Hansen, J. R. Lien, O. Nathan and A. Sperduto, Nuclear Physics A 243, (1975) 100.
[17] J. Jänecke, *Isospin in Nuclear Physics*, edited by D.H. Wilkinson (North-Holland, Amsterdam, 1969), p 297.
[18] K.P. Artemov, *et al.*, Sov. J. Nucl. Phys. **52** (2001) 562.
[19] S. Kubono, Nucl. Phys. **A693** (2001) 221.

Appendix

DESCRIPTION OF THE PROPOSED EXPERIMENT

The experimental setup comprises: (*name the fixed-ISOLDE installations, as well as flexible elements of the experiment*)

Part of the	Availability	Design and manufacturing
Scattering chamber. In place snce 2010	☒ Existing	☒ To be used without any modification
[Part 1 of experiment/ equipment]	☐ Existing	☐ To be used without any modification ☐ To be modified
	☐ New	☐ Standard equipment supplied by a manufacturer ☐ CERN/collaboration responsible for the design and/or manufacturing
[Part 2 of experiment/ equipment]	☐ Existing	☐ To be used without any modification ☐ To be modified
	☐ New	☐ Standard equipment supplied by a manufacturer ☐ CERN/collaboration responsible for the design and/or manufacturing
[insert lines if needed]		

HAZARDS GENERATED BY THE EXPERIMENT (if using fixed installation:) Hazards named in the document relevant for the fixed [COLLAPS, CRIS, ISOLTRAP, MINIBALL + only CD, MINIBALL + T-REX, NICOLE, SSP-GLM chamber, SSP-GHM chamber, or WITCH] installation.

Additional hazards:

Hazards	[Part 1 of experiment/ equipment]	[Part 2 of experiment/ equipment]	[Part 3 of experiment/ equipment]
Thermodynamic and fluidic			
Pressure	No		
Vacuum	1E-6 mbar		
Temperature	No		
Heat transfer	No		
Thermal properties of materials	No		
Cryogenic fluid	None		
Electrical and electromagnetic			
Electricity	50 [V], 1E-6[A]*3		
Static electricity			
Magnetic field	none		
Batteries	☐		
Capacitors	☐		

Ionizing radiation			
Target material	(CH2)n, C		
Beam particle type (e, p, ions, etc)	^{26,30}Mg		
Beam intensity	4E4 pps		
Beam energy	3 MeV/u		
Cooling liquids	No		
Gases	No		
Calibration sources:	☒		
• Open source	☒		
• Sealed source	□ [ISO standard]		
• Isotope	^{241}Am		
• Activity			
Use of activated material:	No		
• Description	□		
• Dose rate on contact and in 10 cm distance	[dose][mSV]		
• Isotope			
• Activity			
Non-ionizing radiation			
Laser	No		
UV light	No		
Microwaves (300MHz-30 GHz)	No		
Radiofrequency (1-300 MHz)	No		
Chemical			
Toxic			
Harmful			
CMR (carcinogens, mutagens and substances toxic to reproduction)			
Corrosive			
Irritant			
Flammable			
Oxidizing			
Explosiveness			
Asphyxiant			
Dangerous for the environment			
Mechanical			
Physical impact or mechanical energy (moving parts)	no		

Mechanical properties (Sharp, rough, slippery)	no		
Vibration	no		
Vehicles and Means of Transport	no		
Noise			
Frequency	no		
Intensity	no		
Physical			
Confined spaces	no		
High workplaces	no		
Access to high workplaces	no		
Obstructions in passageways	no		
Manual handling	no		
Poor ergonomics	no		

Hazard identification:

Average electrical power requirements (excluding fixed ISOLDE-installation mentioned above): [make a rough estimate of the total power consumption of the additional equipment used in the experiment]
4 crates with 500 W power supplies